Supporting Information

Construction of Ru/FeCoP Heterointerface to Drive Dual Active Sites Mechanism for Efficient Overall Water Splitting

Yilin Wang,[a] Yunmei Du,*[b] Ziqi Fu,[a] Jinhong Ren,[b] Yunlei Fu [a] and Lei Wang*[a,b]

[a] College of Chemistry and Molecular Engineering, Qingdao University of Science and Technology, Key Laboratory of Eco-chemical Engineering, Key Laboratory of Optic-electric Sensing and Analytical Chemistry of Life Science, Taishan Scholar Advantage and Characteristic Discipline Team of Eco Chemical Process and Technology, Qingdao 266042, P. R. China.

[b] College of Environment and Safety Engineering, Qingdao University of Science and Technology, Shandong Engineering Research Center for Marine Environment Corrosion and Safety Protection, Qingdao 266042, P. R. China

*E-mail: duyunmeiqust@163.com (Yunmei Du); inorchemwl@126.com (Lei Wang)

DFT calculations

DFT calculations were performed in the Vienna ab initio simulation package (VASP), using the projector augmented wave (PAW) method.The exchange-correlation potential was represented by the Perdew-Burke-Ernzerhof (PBE) functional within the generalized gradient approximation (GGA). All-electron plane-wave basis sets with an energy cutoff of 450 eV, and the convergence tolerances of energy and force are set to $1.0´10^{-5}$ eV/atom $3.0´10^{-2}$ eV/Å, respectively. The *k*-point sampling grid is set to 2×2×1. 15 Å vacuum layer was added to avoid the interaction between adjacent layers. Meanwhile, the DFT-D correction method is used to describe the van der Waals interaction.

The free energy change (ΔG_{H^*}) for adsorptions were determined as follows:

$$\Delta G_{H^*} = \Delta E + \Delta E_{ZPE} - T\Delta S$$

where ΔE is the total energy difference, ΔE_{ZPE} is the zero-point energy change, T is the temperature (T = 298.15 K), and ΔS is the entropy change.

Figures and Tables

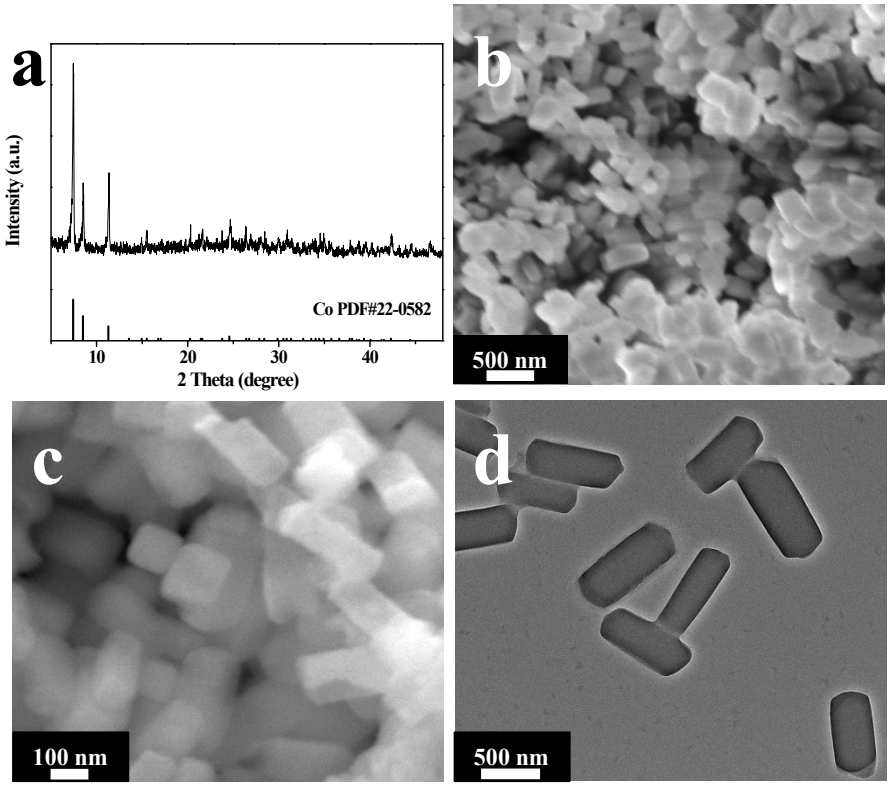

Figure S1 (a) XRD pattern, (b-c) SEM images and (d) TEM image of Co precursor.

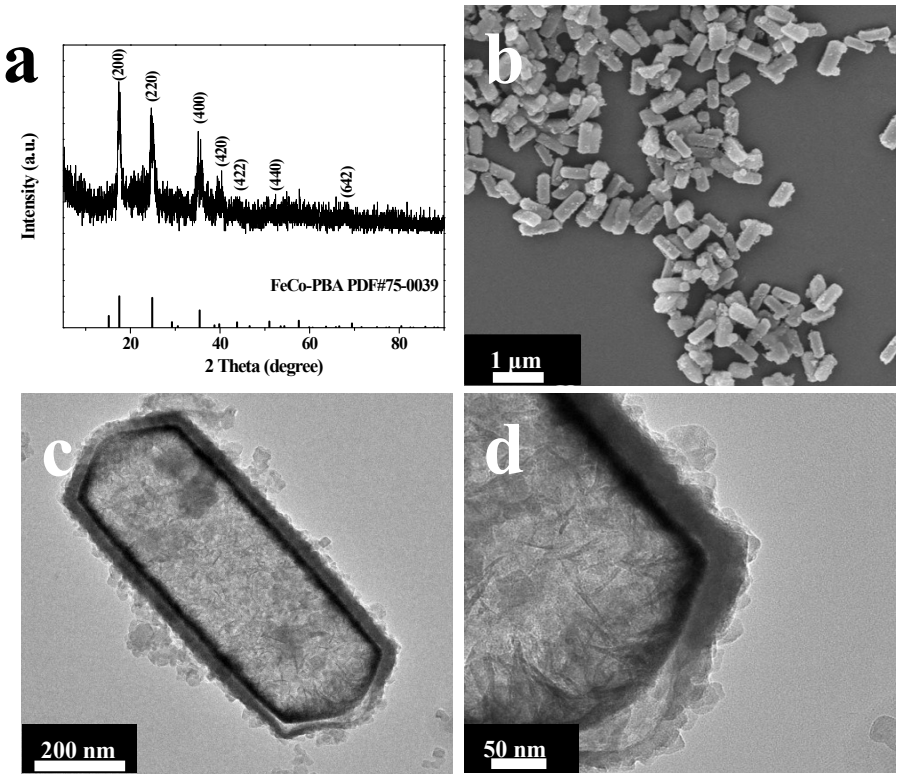

Figure S2 (a) XRD pattern, (b) SEM image and (c-d) TEM images of FeCo-PBA.

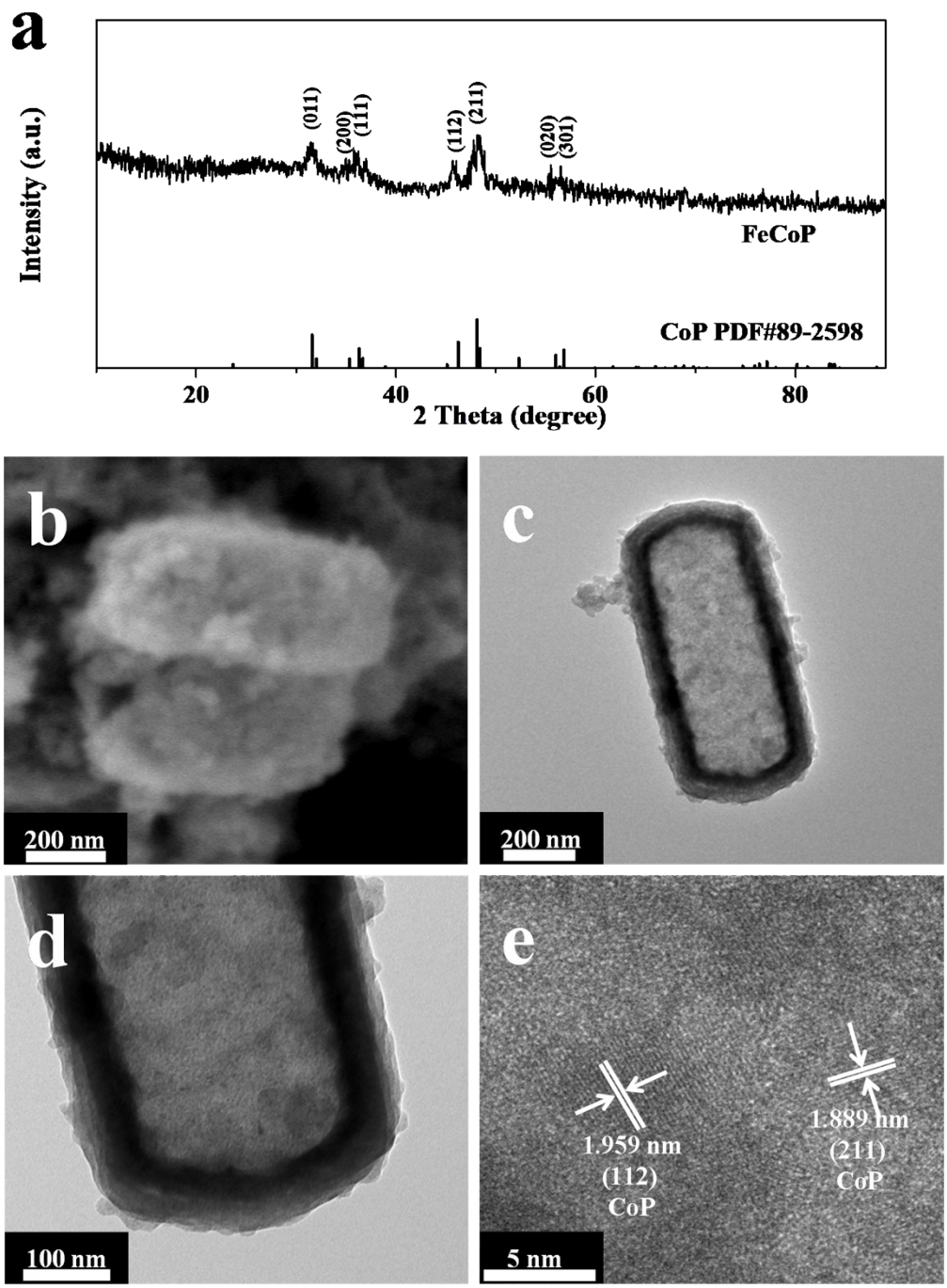

Figure S3 (a) XRD pattern, (b) SEM image, (c-d) TEM images and (e) High-resolution TEM image of FeCoP.

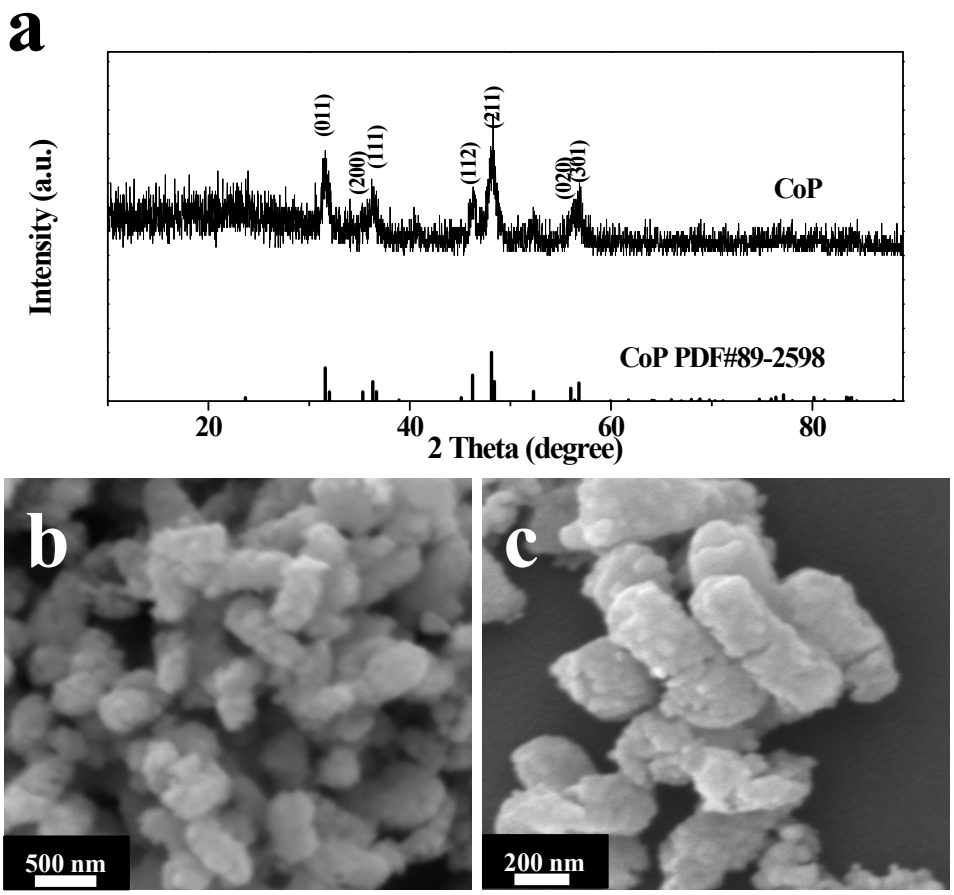

Figure S4 (a) XRD pattern, (b-c) SEM images of CoP.

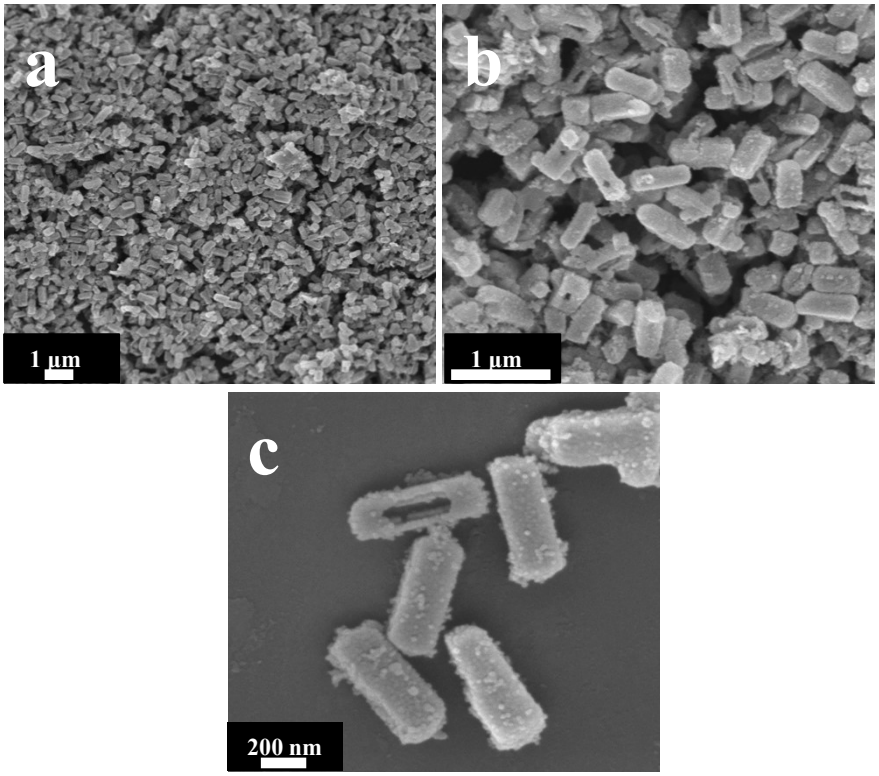

Figure S5 (a-c) SEM images of Ru@FeCoP.

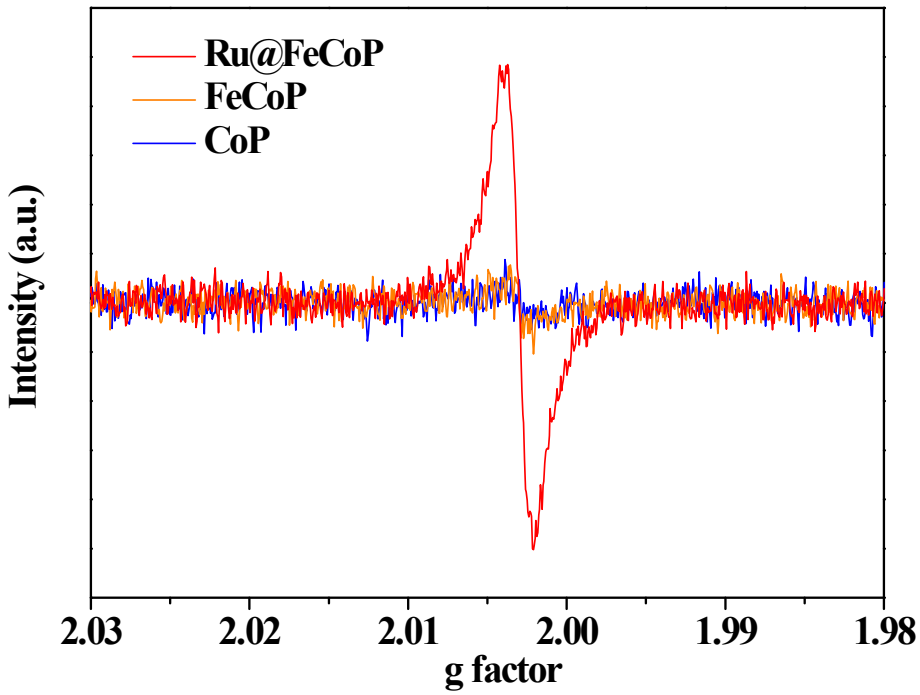

Figure S6 The EPR of Ru@FeCoP, FeCoP, and CoP.

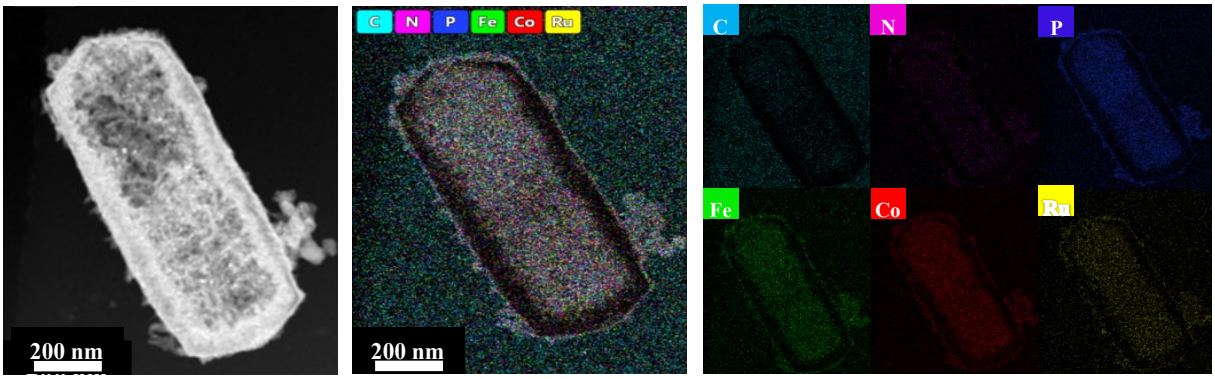

Figure S7 EDX elemental mappings of Ru@FeCoP.

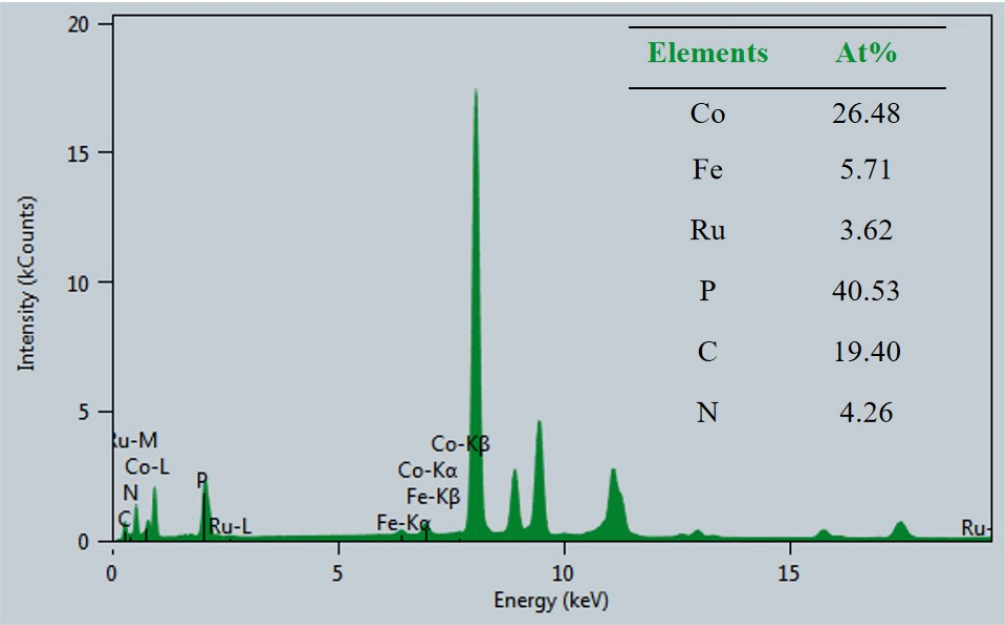

Figure S8 EDX of Ru@FeCoP catalyst.

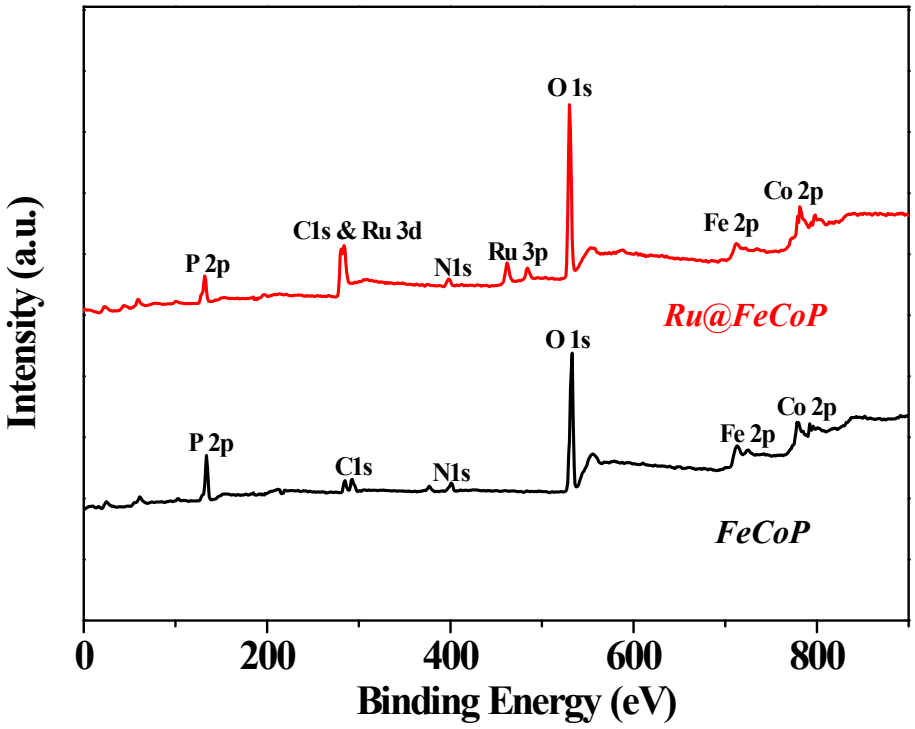

Figure S9 XPS survey spectra of Ru@FeCoP and FeCoP.

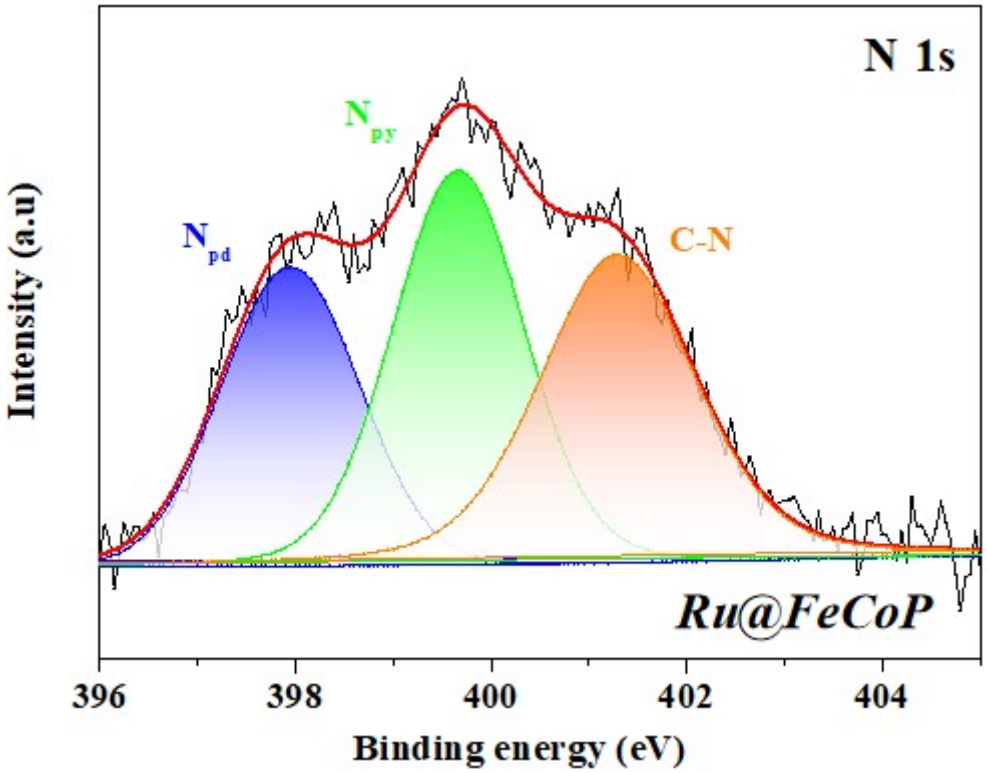

Figure S10 XPS spectra of N 1s in Ru@FeCoP.

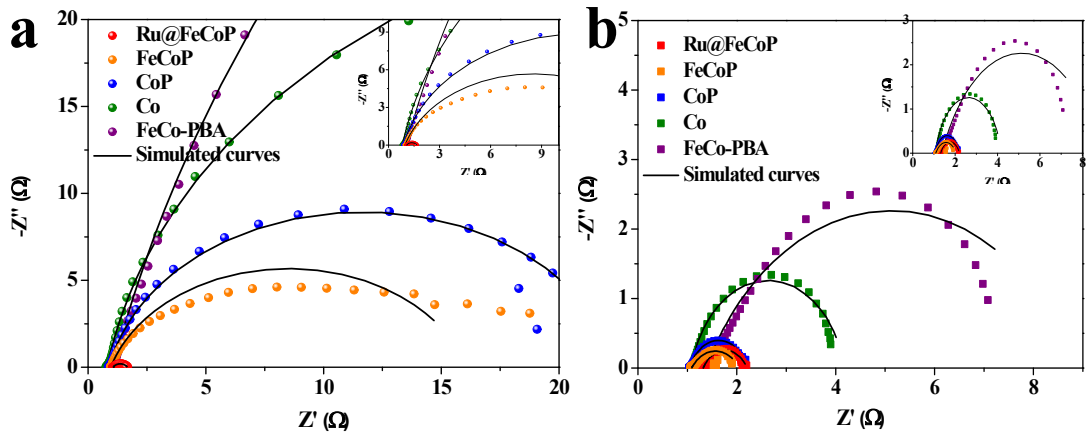

Figure S11 Nyquist plots of Ru@FeCoP, FeCoP, CoP, FeCo-PBA and Co precursor for (a) HER, (b) OER.

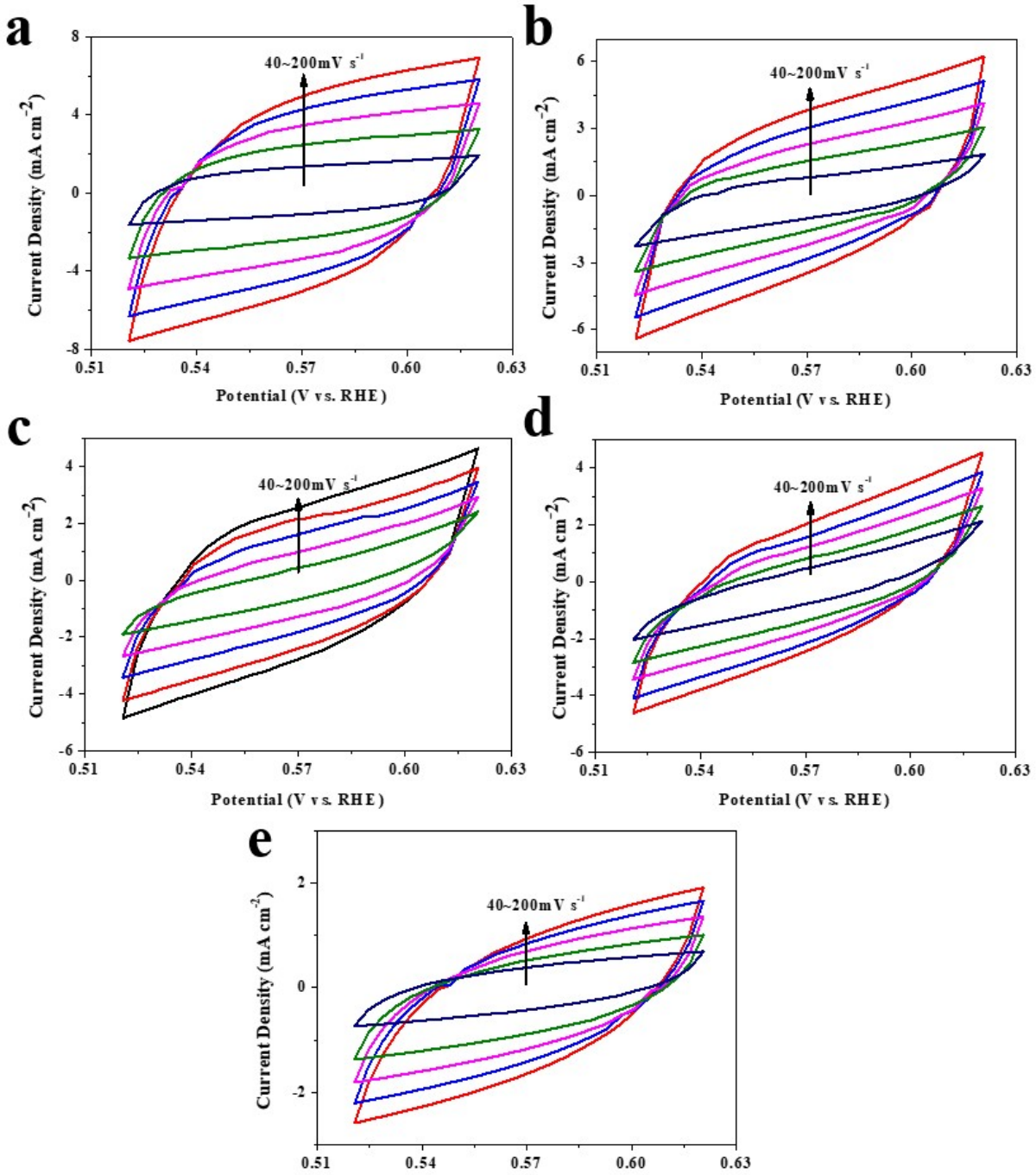

Figure S12 Cyclic voltammetry curves at 0.521~0.621 V vs RHE for (a) Ru@FeCoP, (b) FeCoP, (c) CoP, and (d) Co (e) FeCo-PBA with different scan rates from 40 to 200 mV s^{-1}.

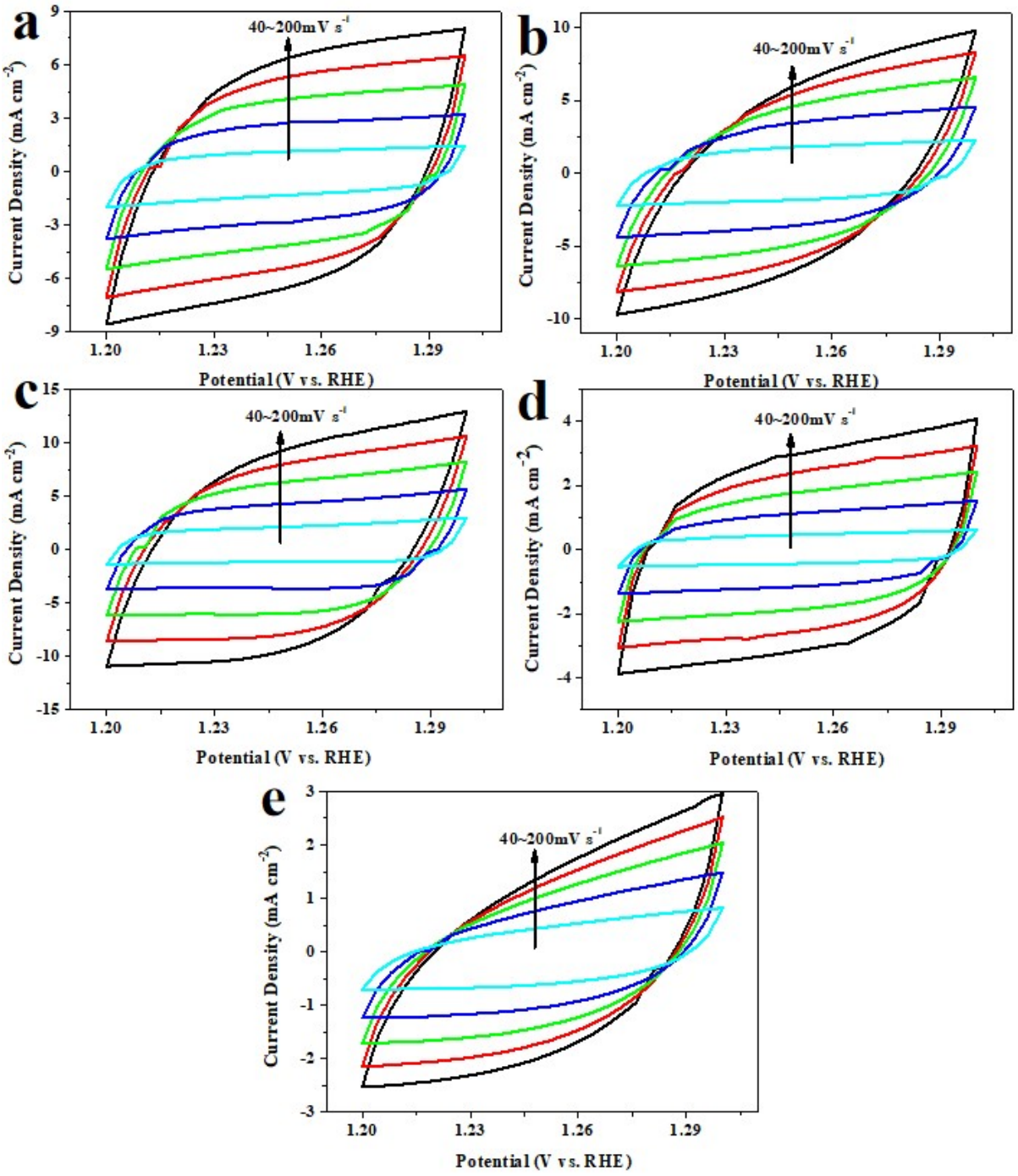

Figure S13 Cyclic voltammetry curves at 1.2~1.3 V vs RHE for (a) Ru@FeCoP, (b) FeCoP, (c) CoP, and (d) Co (e) FeCo-PBA with different scan rates from 40 to 200 mV s^{-1}.

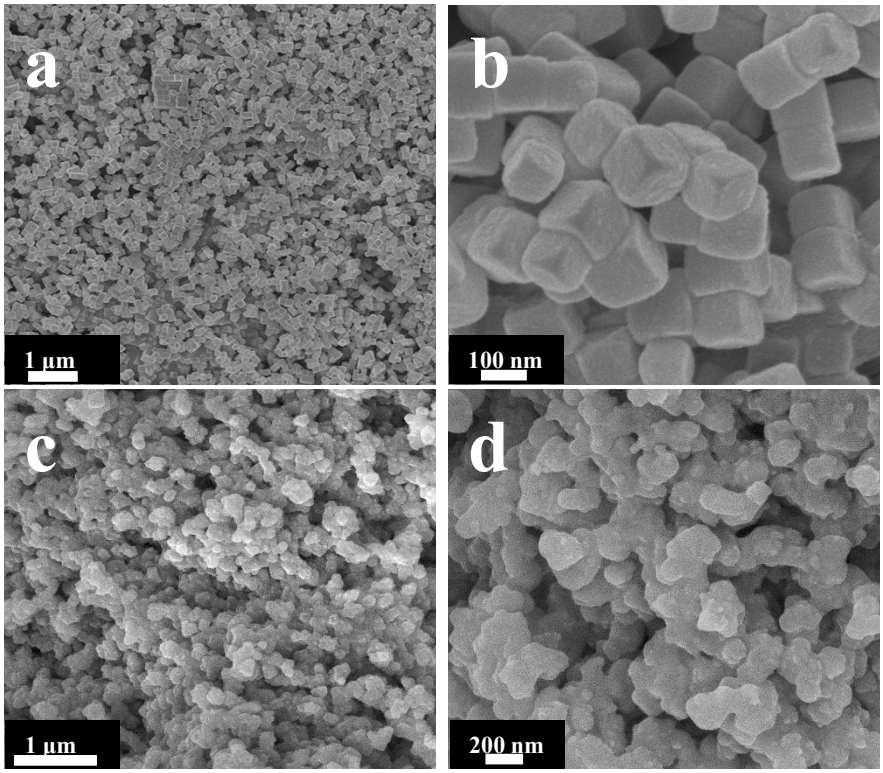

Figure S14 SEM images of (a-b) FeCo-PBA-solid, (c-d) Ru@FeCoP-solid.

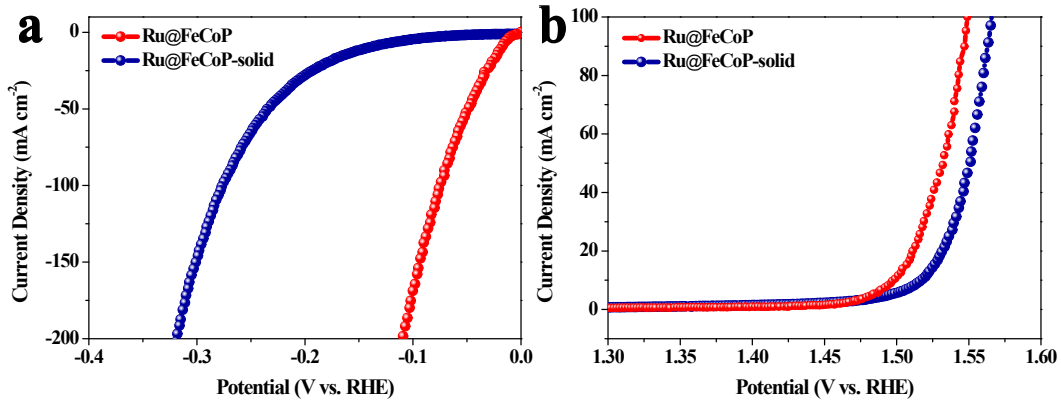

Figure S15 Polarization curves for Ru@FeCoP and Ru@FeCoP-solid of (a) HER, (b) OER.

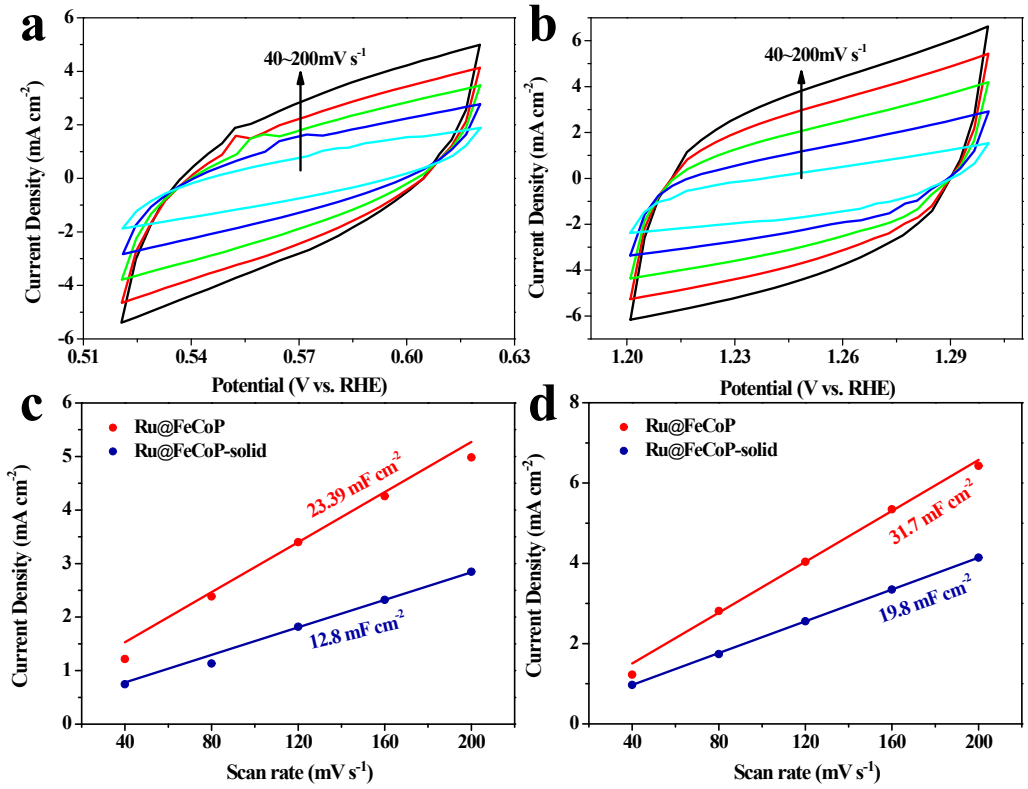

Figure S16 Cyclic voltammetry curves for Ru@FeCoP-solid of (a) HER, (b) OER with different scan rates from 40 to 200 mV s^{-1}, and C_{dl} measurements of (c) HER, and (d) OER of Ru@FeCoP and Ru@FeCoP-solid.

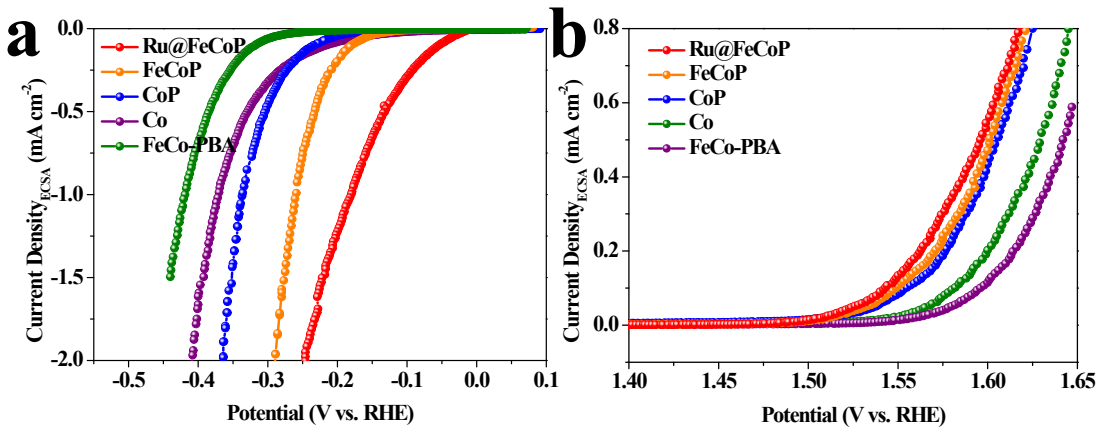

Figure S17 ECSA-normalized (a) HER polarization curves, and (b) OER polarization curves of the Ru@FeCoP, FeCoP, CoP, Co and FeCo-PBA.

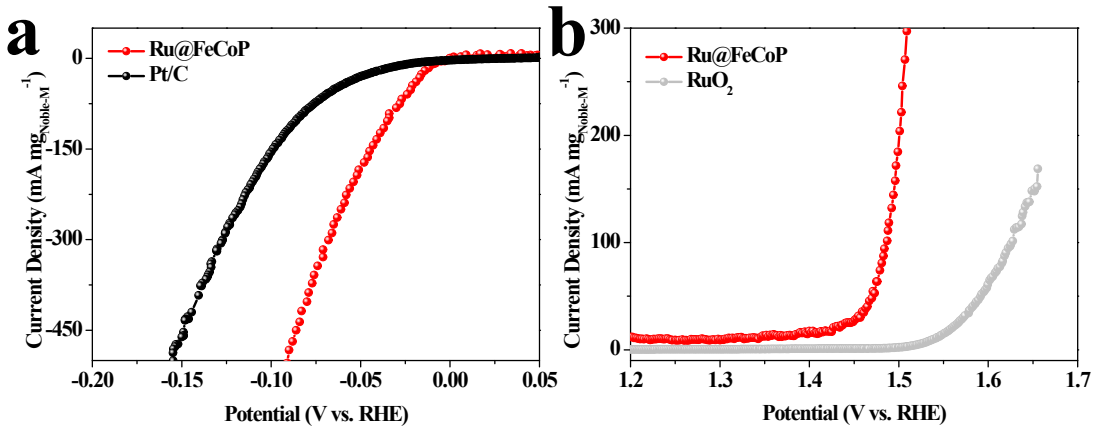

Figure S18 Noble-metal-mass (a) HER polarization curves of Ru@FeCoP and Pt/C, and (b) OER polarization curves of the Ru@FeCoP and RuO_2.

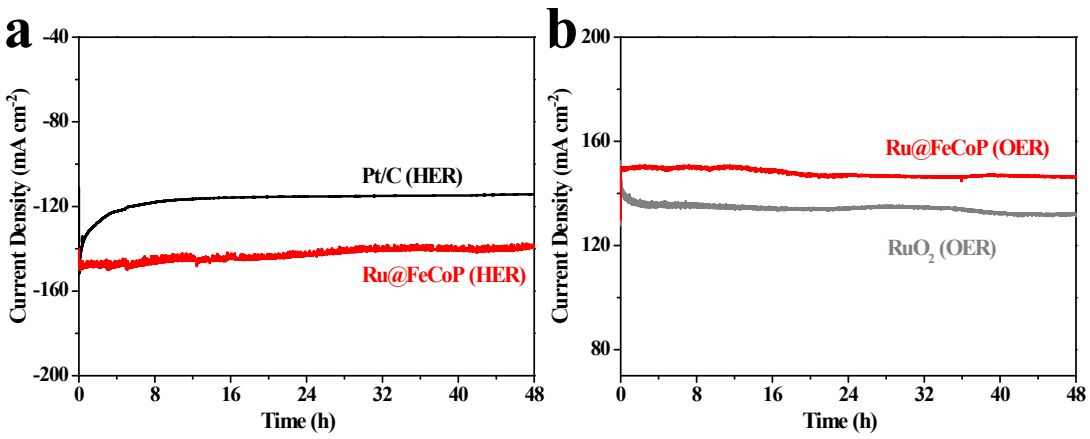

Figure S19 The chronoamperometry test of (a) HER, and (b) OER for Ru@FeCoP, commercial Pt/C, and RuO_2 in 1.0 M KOH.

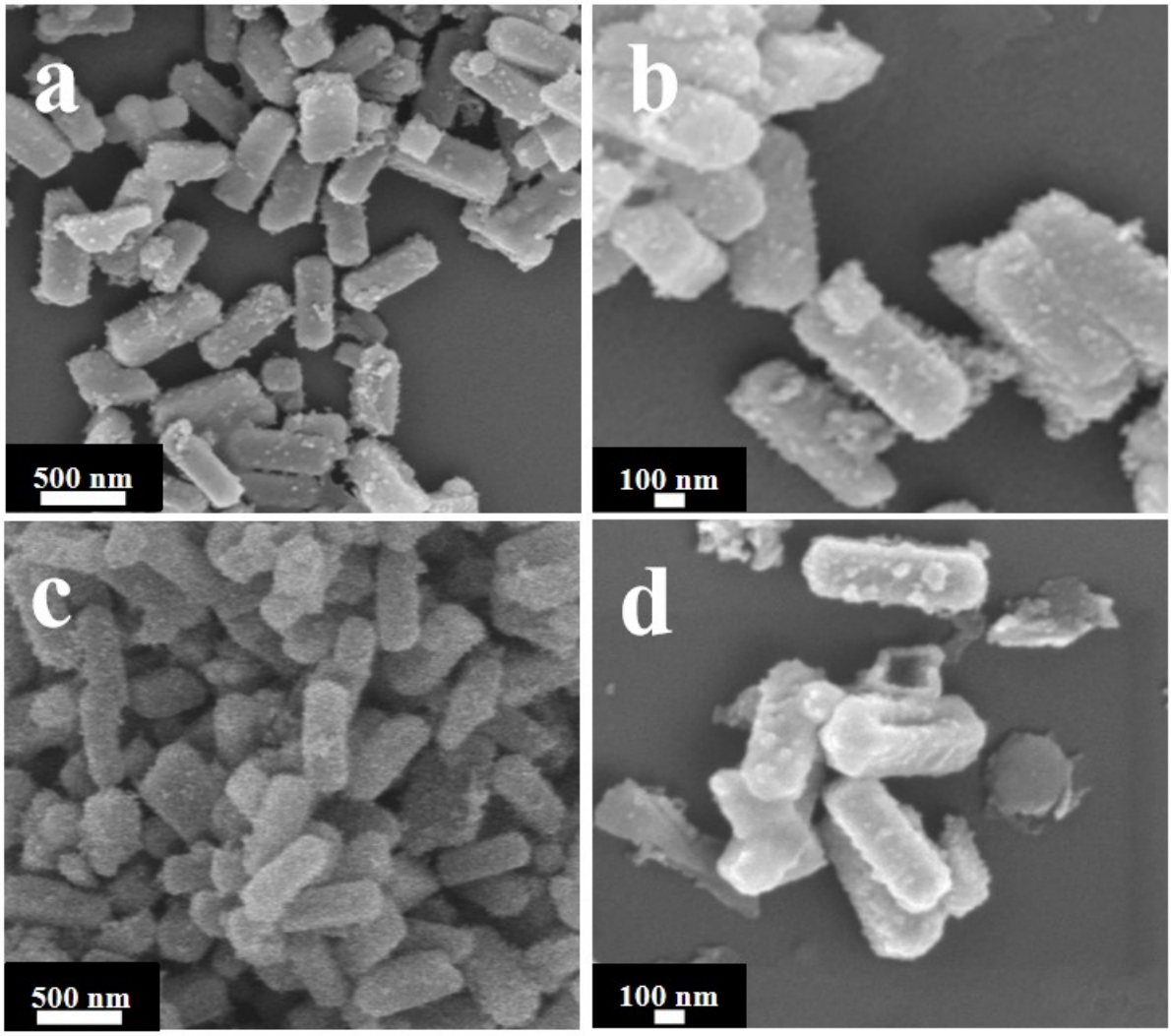

Figure S20 SEM images of Ru@FeCoP (a-b) after HER, and (c-d) after OER.

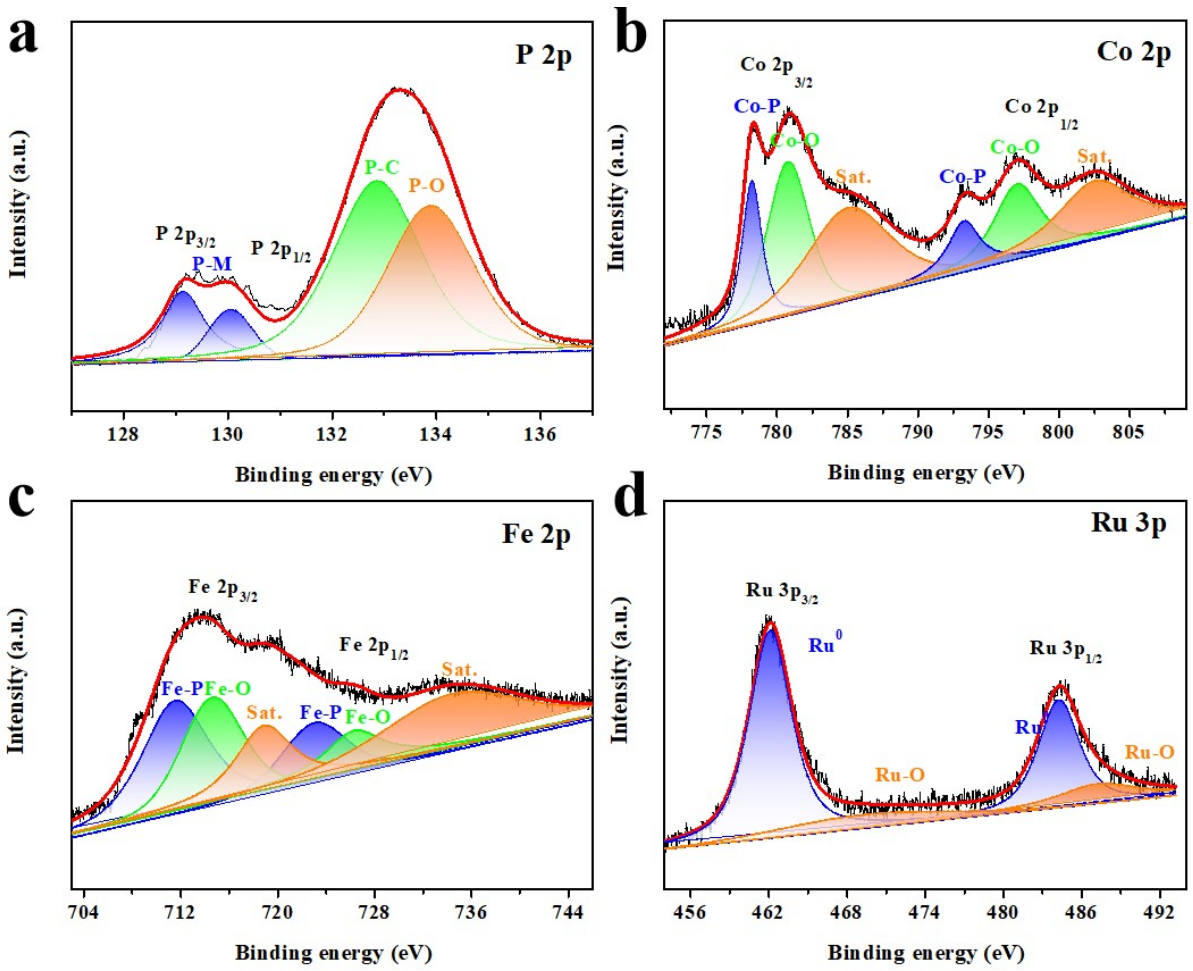

Figure S21 XPS spectra of the Ru@FeCoP after HER stability test: (a) P 2p, (b) Co 2p, (c) Fe 2p, and (d) Ru 3p spectrum.

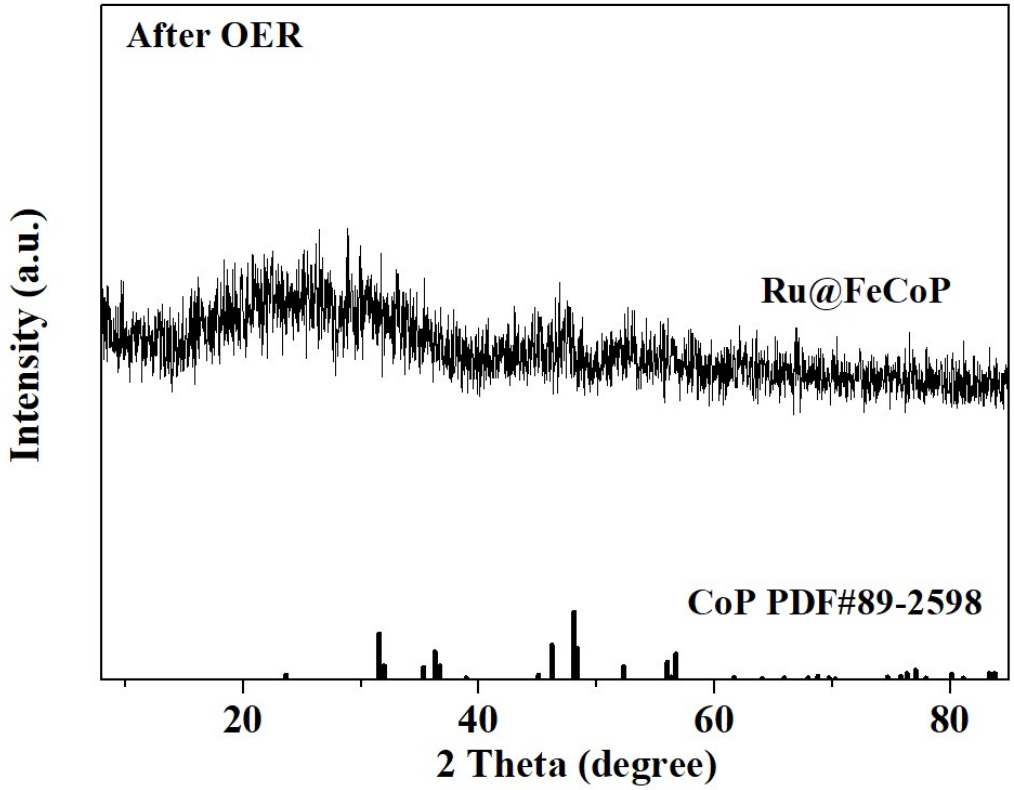

Figure S22 XRD patterns of Ru@FeCoP after OER.

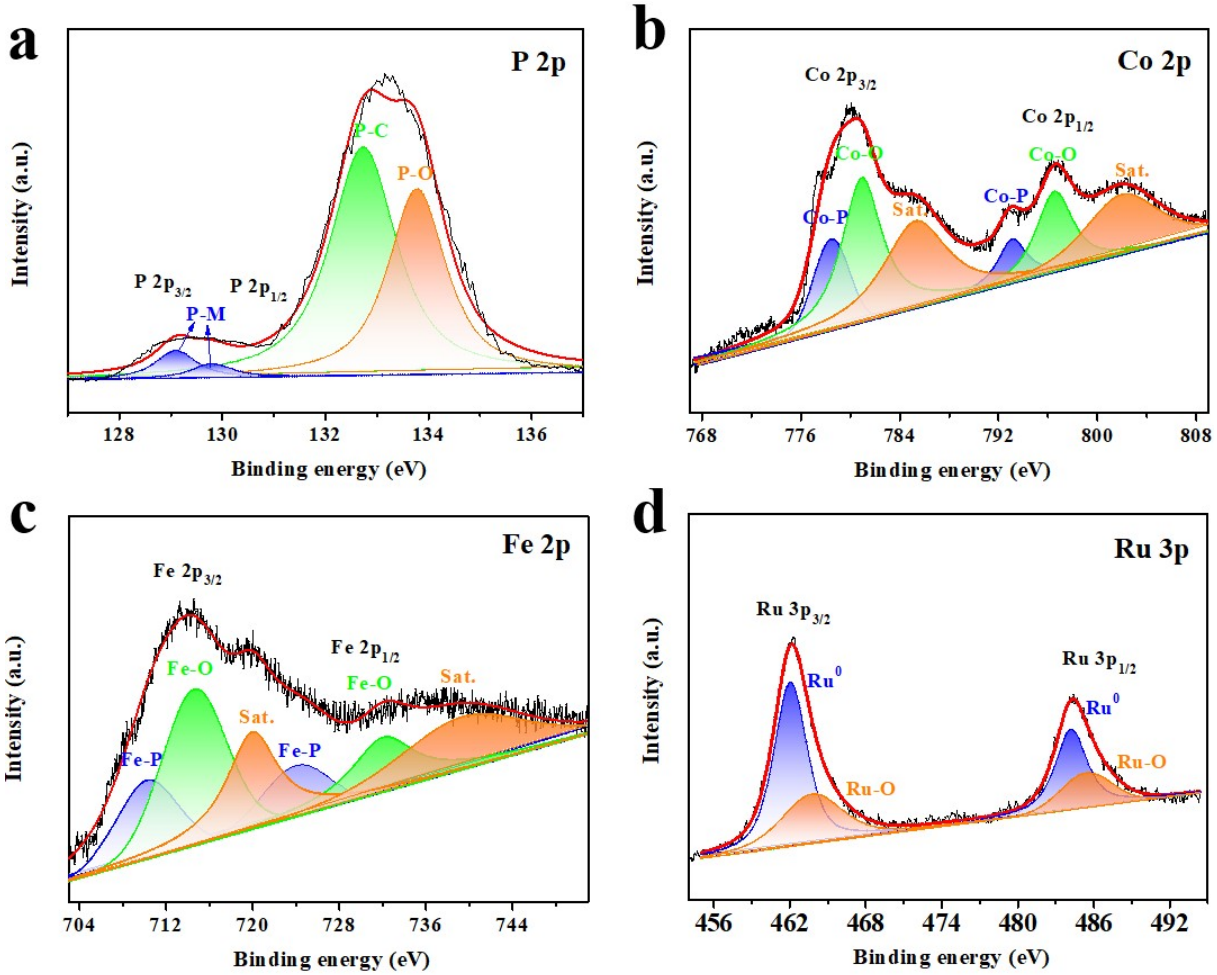

Figure S23 XPS spectra of the Ru@FeCoP after OER stability test: (a) P 2p, (b) Co 2p, (c) Fe 2p, and (d) Ru 3p spectrum.

Table S1 ICP-AES data of Ru@FeCoP.

Elements	**Mass Fraction** **wt.%**
Ru	3.6965
Fe	6.2719
Co	22.5099
P	30.9449

Table S2. Comparison of HER activity between Ru@FeCoP and recently reported noble metal-based electrocatalysts in alkaline conditions.

Electrocatalysts	j (mA cm^{-2})	η (mV)	Tafel slope (mV dec^{-1})	Electrolyte solution	
Ru@FeCoP	10	17.4	31.6	1.0 M KOH	This work
Pt/VS_2	10	77	39.46	1.0 M KOH	S1
Ru-3D NCN	10	17	42	1.0 M KOH	S2
3D RuCu NCs	10	18	59	1.0 M KOH	S3
Ru-MnFeP/NF	10	35	36	1.0 M KOH	S4
RuNiCoP/NF	10	44	45.4	1.0 M KOH	S5
Ru-SAs@N-TC	10	14	58	1.0 M KOH	S6
S-RuP@NPSC	10	90	90.23	1.0 M KOH	S7
Rh_xP/NPC	10	19	36	1.0 M KOH	S8
IrMo NPs	10	38	60	1.0 M KOH	S9
Ru/np-MoS_2	10	30	31	1.0 M KOH	S10
Ru/Co_3O_4 NWs	10	30.96	69.75	1.0 M KOH	S11

Table S3. Comparison of OER activity between Ru@FeCoP and recently reported noble metal-based electrocatalysts in alkaline conditions.

Electrocatalysts	j (mA cm^{-2})	η (mV)	Tafel slope (mV dec^{-1})	Electrolyte solution	Refs.
Ru@FeCoP	10	262	45.7	1.0 M KOH	This work
Ru/N-BP2000-4wt%	10	285	70	1.0 M KOH	S12
Au@$NiCo_2S_4$	10	299	44	1.0 M KOH	S13
Ru-CoNi@NC-2	10	268	75	1.0 M KOH	S14
2D PdIr PNSs	10	285	76.1	1.0 M KOH	S15
Ru-RuP_x-Co_xP	10	291	85.4	1.0 M KOH	S16
RuO_2/Co_3O_4 NBs	10	302	75.77	1.0 M KOH	S17
RuO_2/Co_3O_4	10	305	69	1.0 M KOH	S18
Co-PB/Pt	10	300	68	1.0 M KOH	S19
0.6 Ni-Fe-Pt	10	333	65	1.0 M KOH	S20
Pt-$LiCoO_2$	10	440	82	1.0 M KOH	S21

Table S4. Comparison of electrochemical surface area (ECSA) of Ru@FeCoP catalyst and other comparative samples for HER.

Electrocatalysts	C_{dl} (mF cm^{-2})	C_{DL} (mF)	ECSA (cm^{-2})
Ru@FeCoP	23.39	23.39	584.75
FeCoP	17.78	17.78	444.5
CoP	14.18	14.18	354.5
Co	10.79	10.79	269.75
FeCo-PBA	5.34	5.34	133.5

$C_{DL} = C_{dl} * S$; S=1*1 cm^2; ECSA = C_{DL}/C_s; C_s = 0.04 mF cm^{-2}

Table S5. Comparison of electrochemical surface area (ECSA) of Ru@FeCoP catalyst and other comparative samples for OER.

Electrocatalysts	C_{dl} (mF cm^{-2})	C_{DL} (mF)	ECSA (cm^{-2})
Ru@FeCoP	31.7	31.7	792.5
FeCoP	26.8	26.8	670
CoP	23.1	23.1	577.5
Co	15.5	15.5	387.5
FeCo-PBA	7.06	7.06	176.5

$C_{DL} = C_{dl} * S$; S=1*1 cm^2; ECSA = C_{DL}/C_s; C_s = 0.04 mF cm^{-2}

Table S6. Comparison of overall water splitting activity between Ru@FeCoP‖ Ru@FeCoP and recently reported noble metal-based electrocatalysts in alkaline conditions.

Electrocatalysts	***j*** **(mA cm^{-2})**	***Voltage*** **(mV)**	**Electrolyte solution**	**Refs.**
Ru@FeCoP	10	1.508	1.0 M KOH	This work
O-CoP	10	1.60	1.0 M KOH	S22
S-CoO_x	10	1.63	1.0 M KOH	S23
$Cu_{0.075}Co_{0.925}P$/CP/	10	1.55	1.0 M KOH	S24
NiFeLDH@NiCoP	10	1.57	1.0 M KOH	S25
Co-NC/CF	10	1.65	1.0 M KOH	S26
Ceria/Ni-TMO	10	1.58	1.0 M KOH	S27
V-CoP@a-CeO_2	10	1.56	1.0 M KOH	S28
Fe-Doped Ni-Co-P	10	1.61	1.0 M KOH	S29
NiFeP/SG	10	1.54	1.0 M KOH	S30
CoFe@NiFe/NF	10	1.59	1.0 M KOH	S31

Refs.

1. M. Lu, S. Kong, S. Yan, P. Zhou, T. Yu and Z. Zou, J. Mater. Chem. A, 2022, DOI: 10.1039/D1TA11011J.

2. H. Yoon, H. J. Song, B. Ju and D. W. Kim, *Nano Res.*, 2020, **13**, 2469-2477.

3. Q. Chen, Y. Nie, M. Ming, G Fan, Y. Zhang and J. Hu, *Chin. J. Catal*., 2020, **41**, 1791-1811.

4. Y. Du, W. Wang, H. Zhao, Y. Liu, S. Li and L. Wang, *J. Mater. Chem.,* 2020, **8**, 25165-25172.

5. Y. Zhao, Y. Gao, Z. Chen, Z. Li, T. Ma, Z. Wu and L. Wang, *Appl. Catal. B: Environ.,* 2021, **297**,120395.

6. Y. Wang, G. Qian, Q. Xu, H. Zhang, F. Shen, L. Luo and S. Yin, *Appl. Catal. B: Environ.*, 2021, **286**, 119881.

7. D. H. Kweon, M. S. Okyay, S. J. Kim, J. P. Jeon, H. J. Noh, N. Park, J. Mahmood and J. B. Baek, *Nat. Commun*., 2021, **11**, 1-10.

8. B. Yan, D. Liu, X. Feng, M. Shao and Y. Zhang, *Adv. Funct. Mater.,* 2020, **30**, 2003007.

9. D. Chen, Z. Pu, R. Lu, P. Ji, P. Wang, J. Zhu, C. Lin, H. W. Li, X. Zhou, Z. Hu, F. Xia, J. Wu and S. Mu, *Adv. Energy Mater*., 2020, **10,** 2000814.

10. D. Cao, J. Wang, H. Xu and D. Cheng, *Small*, 2020, **16,** 2000924.

11. P. V. Sarma, T. V. Vineesh, R. Kumar, V. Sreepal, R. Prasannachandran, A. K. Singh and M. M. Shaijumon, *ACS Catal*., 2020, **10,** 6753-6762.

12. Z. Liu, L. Zeng, J. Yu, L. Yang, J. Zhang, X. Zhang, F. Han, L. Zhao, X. Li, H. Liu and W. Zhou, *Nano Energy*, 2021, **85,** 105940.

13. H. Li, M. Zhang, L. Yi, Y, Liu, K. Chen, P. Shao and Z. Wen, *Appl. Catal. B Environ*., 2021, **280**, 119412.

14. X. Liu, F. Liu, J. Yu, G. Xiong, L. Zhao, Y. Sang, S. Zuo, J. Zhang, H. Liu and W. Zhou, *Adv. Sci*., 2020, **7**, 2001526.

15. Q. Qin, H. Jang, L. Chen, G. Nam, X. Liu and J. Cho, *Adv. Energy Mater.*, 2018, **8**, 1801478.

16. A. Yang, K. Su, S. Wang, Y. Wang, X. Qiu, W. Lei and Y. *Tang, Appl. Surf. Sci*., 2020, **510**, 145408

17. J. Guo, X. Zhang, Y. Sun, L. Tang, Q. Liu and X. Zhang, *Chem. Eng*., 2017, **5,** 11577-11583.

18. H. Hu, Farhad M. D, Kazim, Q. Zhang, K. Qu, Z. Yang and W. Cai, *Chemcatchem,* 2019, **11**, 4327-4333.

19. B. Y. Guo, X. Y. Zhang, X. Ma, T. S. Chen, Y. Chen, M. L. Wen, J. F. Qin, J. Nan, Y. M. Chai and B. Dong, *nt. J. Hydrog. Energy*, 2020, **45**, 9575-9582.

20. W. Wang, S. Xi, Y. Shao, W. Sun, S. Wang, J. Gao, C. Mao, X. Guo and G. Li, *Chem. Eng*., 2019, **7**, 17227-17236.

21. M. Fu, Q. Zhang, Y. Sun, G. N, X. Fan, H. Wang, H. Lu, Y. Zhang and H. Wang, *Int. J. Hydrog. Energy*, 2020, **45**, 20832-20842.

22. S22 G. Zhou, M. Li, Y. Li, H. Dong, D. Sun, X. Liu, L. Xu, Z. Tian and Y. Tang, *Adv. Funct. Mater.* 2020*,* **30**, 1905252.

23. X. Yu, Z. Y. Yu, X. L. Zhang, P. Li, B. Sun, X. Gao, K. Yan, H. Liu, Y. Duan, M. R. Gao, G. Wang and S. H. Yu, *Nano Energy*, 2020, **71**, 104652.

24. L. Yan, B. Zhang, J. Zhu, S. Zhao, Y. Li, B. Zhang, J. Jiang, X. Ji, H. Zhang and P. K. Shen, *J. Mater. Chem. A*, 2019, **7**, 14271-14279.

25. H. Zhang, X. Li, A. Hähnel, V. Naumann, C. Lin, S. Azimi, S. L. Schweizer, A. W. Maijenburg and R. B. Wehrspohn, *Adv. Funct. Mater.*, 2018, **28**, 1706847.

26. H. Huang, S. Zhou, C. Yu, H. Huang, J. Zhao, L. Dai and J. Qiu, *Energy Environ. Sci.,* 2020*,* **13**, 545-553.

27. X. Long, H. Lin, D. Zhou, Y. An and S. Yang, *ACS Energy Lett.* 2018*,* **3**, 290-296.

28. L. Yang, R. Liu, L. Jiao, *Adv. Funct. Mater.,* 2020*,* **30**, 1909618.

29. M. Guo, S. Song, S. Zhang, Y. Yan, K. Zhan, J. Yang and B. Zhao, *ACS Sustain. Chem. Eng,.* 2020, **8**, 7436-7444

30. R. Q. Li, B. L. Wang, T. Gao, R. Zhang, C. Xu, X. Jiang, J. Zeng, Y. Bando, P. Hu, Y. Li and X. B. Wang, *Nano Energy,* 2020, **58**, 870-876.

31. R. Yang, Y. Zhou, Y. Xing, D. Li, D. Jiang, M. Chen, W. Shi and S. Yuan, *Appl. Catal. B,* 2019, **253**, 131-139.